Article

Photochemical Strategies for the Synthesis of Gold Nanoparticles from Au(III) and Au(I) Using Photoinduced Free Radical Generation

M. Luisa Marin, Katherine L. McGilvray, and Juan C. Scaiano

J. Am. Chem. Soc., **2008**, 130 (49), 16572-16584 • DOI: 10.1021/ja803490n • Publication Date (Web): 17 November 2008

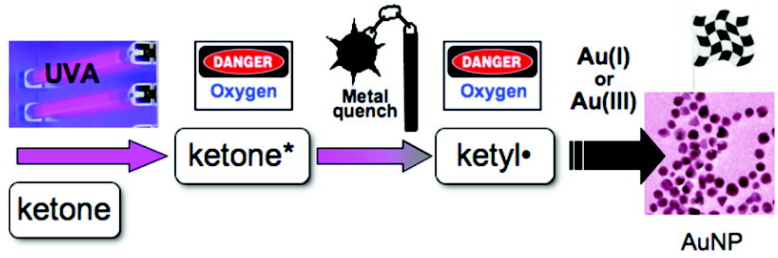

More About This Article

Additional resources and features associated with this article are available within the HTML version:

- Supporting Information
- Access to high resolution figures
- Links to articles and content related to this article
- Copyright permission to reproduce figures and/or text from this article

View the Full Text HTML

J|A|C|S
ARTICLES

Published on Web 11/17/2008

Photochemical Strategies for the Synthesis of Gold Nanoparticles from Au(III) and Au(I) Using Photoinduced Free Radical Generation

M. Luisa Marin,[†] Katherine L. McGilvray,[‡] and Juan C. Scaiano*[,‡]

Instituto de Tecnología Química CSIC-UPV, Universidad Politécnica de Valencia, Av. de los Naranjos s/n, 46022 Valencia, Spain, and Centre for Catalysis Research and Innovation, Department of Chemistry, University of Ottawa, 10 Marie Curie, Ottawa K1N 6N5, Canada

Received May 10, 2008; Revised Manuscript Received September 15, 2008; E-mail: tito@photo.chem.uottawa.ca

Abstract: A comprehensive study of the ketone-photoinduced formation of gold nanoparticles (AuNPs) from gold ions in aqueous and micellar solution has been carried out. Ketones are good photosensitizers for nanoparticle synthesis not because of the energy they can absorb or deliver but rather because of the reducing free radicals they can generate; thus, efficient nanoparticle generation requires a careful selection of substrates and experimental conditions to ensure that free-radical generation occurs with high quantum efficiency and that gold ion precursors do not cause UV screening of the organic photosensitizers. A key consideration in achieving AuNP synthesis with short exposure times is minimizing excited-state quenching by gold ions; this can be achieved by temporal or spatial segregation or a combination of the two. Temporal segregation can be accomplished by using unimolecular precursors, such as benzoins, that yield ketyl radicals from triplet precursors with lifetimes of a few nanoseconds. Spatial segregation can be achieved by using self-assembled structures such as micelles. In this case, the process can be assisted by selecting ketones with n,π^* triplet states and by adding good hydrophobic hydrogen donors such as 1,4-cyclohexadiene. Systems involving bimolecular reactions of ketones are catalytic in that the ketone is recovered at the end of the reductive process. Rate constants have been determined for the quenching of excited triplets and for the scavenging of ketyl radicals by Au(I) and Au(III); in general, these values are within an order of magnitude of the rate constant for diffusion control. This article provides a paradigm for the photochemical production of nanoparticles of gold and other metal ions that highlights ten aspects that must be considered in order to design successful photochemical systems for nanoparticle generation.

Introduction

In recent years, colloidal gold nanoparticles (AuNPs) have been the subject of strong interest in areas of materials science, biotechnology, and organic chemistry for their function as molecular markers and their use in diagnostic imaging and catalysis.[1−3] Their synthesis has primarily been performedf using thermal methods under a variety of conditions, including traditional citrate reduction[4] and the widely employed Brust−Schiffrin method of two-phase synthesis with thiol stabilization.[5]

The photochemical synthesis of metal nanoparticles offers the possibility of controlling the rate of nanoparticle formation as well as the spatial and temporal control that characterizes many photochemical reactions.[6−8] However, some photochemical methods of nanoparticle and nanostructure synthesis involving ultraviolet exposure suffer from the need for long irradiation times. In a recent report from our laboratory,[9] we have shown that inefficient photochemical synthesis of metal nanoparticles can simply reflect extensive quenching of excited-state precursors by the transition-metal ions that are in turn the nanoparticle precursors. For example, Ag(I) can quench the excited states of carbonyl compounds with rate constants approaching the diffusion-controlled limit.[10] In fact, concerns about metal ion quenching are far from new.[11] In principle, quenching problems can be circumvented by designing systems with temporal or spatial segregation of the photoinduced processes required for metal ion reduction and avoidance of precursor quenching events; in this contribution, we evaluate strategies that facilitate efficient photochemical synthesis of AuNPs and should also apply to other systems leading to metal nanoparticles.

[†] Universidad Politécnica de Valencia.
[‡] University of Ottawa.

(1) Corma, A.; Garcia, H. *Chem. Soc. Rev.* **2008**, *37*, 2096.
(2) Burda, C.; Chen, X.; Narayanan, R.; El-Sayed, M. A. *Chem. Rev.* **2005**, *105*, 1025.
(3) Zhu, J.; Lines, B. M.; Ganton, M. D.; Kerr, M. A.; Workentin, M. S. *J. Org. Chem.* **2008**, *73*, 1099.
(4) Turkevich, J.; Stevenson, P. C.; Hiller, J. *Discuss. Faraday Soc.* **1951**, *11*, 55.
(5) Brust, M.; Walker, M.; Bethell, D.; Schiffrin, D. J.; Whyman, R. *J. Chem. Soc., Chem. Commun.* **1994**, 801.
(6) Dong, S.; Tang, C.; Zhou, H.; Zhao, H. *Gold Bull.* **2004**, *37*, 187.
(7) Esumi, K.; Matsumoto, T.; Seto, Y.; Yoshimura, T. *J. Colloid Interface Sci.* **2005**, *284*, 199.
(8) (a) Krylova, G. V.; Eremenko, A.; Smirnova, N.; Eustis, S. *Theor. Exp. Chem.* **2005**, *41*, 365. (b) Majima, T.; Sakamoto, M.; Tachikawa, T.; Fujitsuka, M. *Chem. Phys. Lett.* **2006**, *420*, 90.
(9) McGilvray, K. L.; Decan, M. R.; Wang, D.; Scaiano, J. C. *J. Am. Chem. Soc.* **2006**, *128*, 15980.
(10) Scaiano, J. C.; Aliaga, C.; Maguire, S.; Wang, D. *J. Phys. Chem. B* **2006**, *110*, 12856.
(11) Hammond, G. S.; Foss, R. P. *J. Phys. Chem.* **1964**, *68*, 3739.

 10.1021/ja803490n CCC: $40.75

Scheme 1. Photodecomposition Mechanism for I-2959 and Multistep Reduction of Au(III)[9]

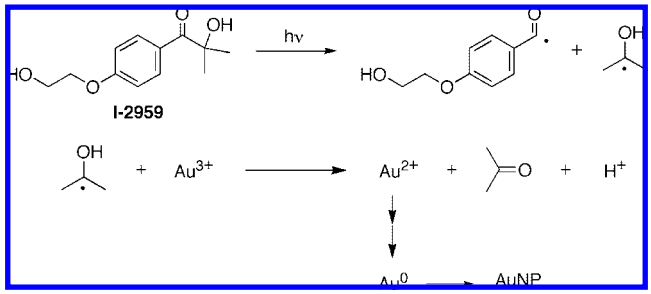

Scheme 2. Production of Ketyl Radicals in the Photodecomposition of **1** and **2**

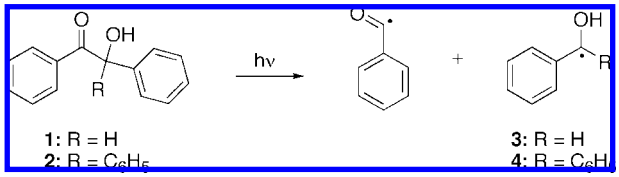

The reducing species involved in metal ion reduction are frequently ketyl radicals, which have been well-established as powerful reducing agents;[12,13] in fact, the redox potentials of ketyl radicals are such that all stages of gold ion reduction are thermodynamically favorable.[14] These reactive intermediates can be generated photochemically in intermolecular reactions involving triplet ketones[15] as well as by the careful selection of intramolecular radical generators such as benzoins.[7,16,17] For example, a ketyl radical (formally derived from 2-propanol) can be readily produced by photolysis of the substituted water-soluble benzoin Irgacure 2959 (I-2959), a photoinitiator produced by Ciba, as illustrated in Scheme 1.[9,17]

The efficiency of the photoprocesses in Scheme 1 is such that upon exposure to >320 nm UV light, AuNP formation can be accomplished in a matter of minutes.[9] This is largely a consequence of the very short (11 ns)[17] triplet lifetime of I-2959, which in turn reflects a very efficient Norrish type-I photocleavage. Thus, on this time scale, the precursors behave as formally "instantaneous" sources of ketyl radicals with a quantum efficiency of 0.29.[17] We have investigated the use of I-2959 as well as the hydrophobic ketones benzoin (**1**) and α-phenylbenzoin (**2**) employed to generate AuNPs very efficiently in micellar solutions (Scheme 2). Our choice of **2** as a precursor evolved from our interest in using laser flash photolysis techniques to study the evolution and initial rates of reduction. Techniques that probe the dynamics of the electron-transfer reactions between ketyl radicals and gold ions are possible as a result of the production of the readily detectable[18] benzophenone ketyl radical upon photocleavage.[19] A comparison

Scheme 3. Intermolecular Photoreduction of Ketones as a Strategy for Ketyl Radical Generation and the Three Ketones Used in This Work

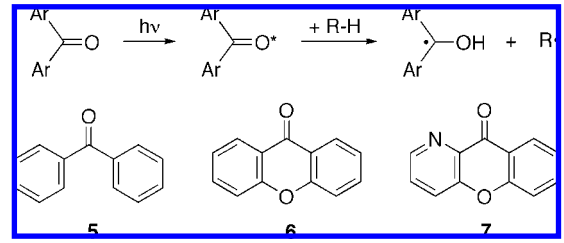

of Au(III) with Au(I) further reveals different time evolutions as well as formation of particles with different average dimensions.

The radical-generating strategies described above refer to one of the two approaches followed in this contribution, namely, temporal separation of the radical-generating processes from the reduction of gold ions, which is achieved by using unimolecular precursors with short triplet lifetimes and good absorption in the UVA region (315−400 nm). A second strategy involves spatial segregation, which is accomplished by placing the radical generators in compartmentalized systems, as achieved in our examples by use of aqueous micelles. In an earlier example involving silver nanoparticles (AgNPs), we tested the idea of spatial reactant segregation by using benzophenone as the absorbing chromophore as well as the hydrogen abstractor leading to ketyl radical formation.[10] The benzophenone triplet state has n,π^* character and is known to react in ways that mimic alkoxyl radicals.[20] Segregation was achieved by using sodium dodecyl sulfate (SDS) micelles. Addition of 1,4-cyclohexadiene, an exceptionally good hydrogen donor,[21,22] helped minimize triplet-state quenching by Ag^+. This strategy is illustrated in Scheme 3 for the aromatic ketones examined in this work. These ketones were selected because of their absorption properties and because their triplet excited states include examples with n,π^* and π,π^* character.[15,23−26]

Currently there is considerable interest in the influence of gold ions and AuNPs on the radicals formed in Norrish type-I and type-II reactions,[27] including their applications in organic synthesis.[3,28,29] The strategies of temporal and spatial segregation do not need to operate independently. Thus, in this work, ketones **1** and **2** were used in micelles; beyond segregation, this helped

(12) (a) Small, R. D.; Scaiano, J. C. *J. Phys. Chem.* **1977**, *81*, 828. (b) Small, R. D., Jr.; Scaiano, J. C. *J. Phys. Chem.* **1977**, *81*, 2126.
(13) Henglein, A.; Meisel, D. *Langmuir* **1998**, *14*, 7392.
(14) Gachard, E.; Remita, H.; Khatouri, J.; Keita, B.; Nadjo, L.; Belloni, J. *New J. Chem.* **1998**, *22*, 1257.
(15) Scaiano, J. C. *J. Photochem.* **1973−1974**, *2*, 81.
(16) (a) Ledwith, A.; Russel, P. J.; Sulcliffe, J. H. *J. Chem. Soc., Perkin Trans.* **1972**, 1925. (b) Colley, C. S.; Grills, D. C.; Besley, N. A.; Jockusch, S.; Matousek, P.; Parker, A. W.; Towrie, M.; Turro, N. J.; Gill, P. M. W.; George, M. W. *J. Am. Chem. Soc.* **2002**, *124*, 14952. (c) Eichler, J.; Herz, C. P.; Naito, I.; Schnabel, W. *J. Photochem.* **1980**, *12*, 225.
(17) Jockusch, S.; Landis, M. S.; Freiermuth, B.; Turro, N. J. *Macromolecules* **2001**, *34*, 1619.
(18) Chatgilialoglu, C. In *Handbook of Organic Photochemistry*; Scaiano, J. C., Ed.; CRC Press: Boca Raton, FL, 1989; Vol. II, p 3.
(19) Small, R. D., Jr.; Scaiano, J. C. *J. Am. Chem. Soc.* **1978**, *100*, 296.
(20) Walling, C.; Gibian, M. J. *J. Am. Chem. Soc.* **1965**, *87*, 3361.
(21) Paul, H.; Small, R. D., Jr.; Scaiano, J. C. *J. Am. Chem. Soc.* **1978**, *100*, 4520.
(22) Wong, P. C.; Griller, D.; Scaiano, J. C. *J. Am. Chem. Soc.* **1982**, *104*, 5106.
(23) Coenjarts, C.; Scaiano, J. C. *J. Am. Chem. Soc.* **2000**, *122*, 3635.
(24) Scaiano, J. C. *J. Am. Chem. Soc.* **1980**, *102*, 7747.
(25) Scaiano, J. C.; Selwyn, J. C. *Can. J. Chem.* **1981**, *59*, 2368.
(26) Scaiano, J. C.; Weldon, D.; Pliva, C. N.; Martínez, L. J. *J. Phys. Chem. A* **1998**, *102*, 6898.
(27) (a) Aprile, C.; Boronat, M.; Ferrer, B.; Corma, A.; Garcia, H. *J. Am. Chem. Soc.* **2006**, *128*, 8388. (b) Kell, A. J.; Alizadeh, A.; Yang, L.; Workentin, M. S. *Langmuir* **2005**, *21*, 9741. (c) Kell, A. J.; Stringle, D. L. B.; Workentin, M. S. *Org. Lett.* **2000**, *2*, 3381. (d) Kell, A. J.; Workentin, M. S. *Langmuir* **2001**, *17*, 7355. (e) Kell, A. J.; Donkers, R. L.; Workentin, M. S. *Langmuir* **2005**, *21*, 735.
(28) (a) Zhu, J.; Ganton, M. D.; Kerr, M. A.; Workentin, M. S. *J. Am. Chem. Soc.* **2007**, *129*, 4904. (b) Zhu, J.; Kell, A. J.; Workentin, M. S. *Org. Lett.* **2006**, *8*, 4993.
(29) Ionita, P.; Conte, M.; Gilbert, B. C.; Chechik, V. *Org. Biomol. Chem.* **2007**, *5*, 3504.

overcome solubility problems. Furthermore, ketones **5**−**7** were also used in conjunction with a hydrogen donor, since the surfactants themselves are only modest hydrogen donors.[30] Several spectroscopic and imaging techniques have been employed. While we examine particle size, stability, and dispersity, the main goal of this contribution is to establish strategies that can facilitate photochemical synthesis of nanoparticles; there is abundant literature on recipes and techniques to reduce particle polydispersity.[2,31,32]

Results

This section is subdivided into the use of unimolecular and bimolecular initiators; the former also includes our comparison of Au(III) and Au(I) as Au(0) precursors. We have also examined the quenching of carbonyl triplet states by gold ions and the scavenging of ketyl radicals using laser flash photolysis techniques. The nature of these experiments is such that they require a significant "prequenching" lifetime for the transient species being examined; thus, we have examined radical scavenging using unimolecular precursors and triplet-state quenching using some of the ketones shown in Scheme 3.

Unimolecular Radical Generation. The benzoins studied here were chosen for their fast and efficient photodissociation to generate reducing ketyl radicals. The excited triplet lifetimes of these precursors have been reported to be approximately 10−20 ns,[17] which is short enough to result in rates of photodissociation approaching 10^8 s^{-1} for triplet states with n,π^* character, with overall efficiencies just below 0.4 for the generation of ketyl radicals. Furthermore, **2** was selected because it provides the ability to study the growth and decay of the benzophenone-like reactive intermediates via laser flash photolysis upon interaction with the auric salt.

Optimization of AuNP Synthesis Conditions Using Unimolecular Precursors. Gold nanoparticles were prepared in (1-hexadecyl)trimethylammonium chloride (CTAC) positively charged micelles using substituted benzoins as reducing agents; independent experiments suggested that better nanoparticles were prepared under these conditions than when using negatively charged micelles, specifically sodium dodecyl sulfate (SDS) (see the Supporting Information). Previous reports[33] have indicated that 253.7 nm photolysis of various surfactants can effectively cause reduction of metal salts at prolonged irradiation times; however, no nanoparticles were generated with the working concentrations and UVA irradiation conditions employed in this contribution. Particles prepared using CTAC produced a blue-shifted and narrower surface-plasmon band (SPB) relative to particles prepared with SDS at an equivalent concentration above the respective critical micelle concentration. Different experimental parameters were investigated in order to optimize the preparation of AuNPs. The first experiments were performed using commercially available **1**, in addition to our earlier work with I-2959.[9] In preliminary work, both (1-hexadecyl)trimethylammonium bromide (CTAB) and CTAC were tested as sources of positively charged micelles at a concentration of 7 mM; however, during attempts to dissolve Au(III) in CTAB, an orange color appeared that never changed to the characteristic pink color of AuNPs upon irradiation in the presence of benzoin.

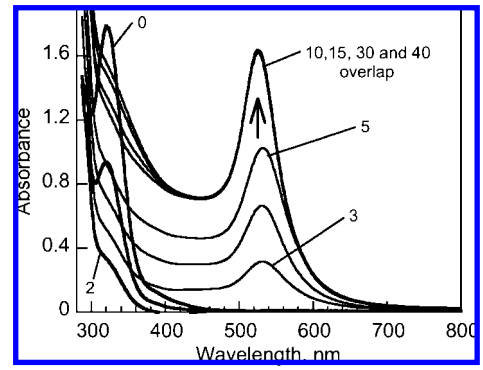

Figure 1. UV−vis absorbance spectra as AuNPs were generated in a deaerated solution containing 1.0 mM **1**, 0.3 mM $HAuCl_4$, and 66 mM CTAC upon exposure to six UVA lamps in a Luzchem photoreactor. Spectra were recorded at 1 min intervals for the first 5 min and then at 10, 15, 30, and 60 min; numeric labels in the graph show representative exposure times.

Under these conditions, the absorbance of I-2959 is masked by absorbance of the CTAB−$AuCl_4^-$ complex, thus inhibiting excitation of the chromophore and generation of the reducing agent (see the Supporting Information). Alternatively, when CTAC micelles were used, AuNPs were readily obtained, as revealed by the formation of the typical SPB. CTAC also has the advantage that only one type of halide (Cl^-) is involved.

More concentrated CTAC micelles were used to check the stability and yield of the AuNPs. In fact, when the CTAC concentration was increased to 66 mM, the yield of nanoparticle formation was higher. Increasing the concentration of both Au(III) and **1** while keeping the 1-to-3 stoichiometric ratio constant led to the formation of less-stable nanoparticles, as dilute conditions are common in various successful nanoparticle syntheses.[2] Studies with benzoins **1** and **2** led to optimized experimental conditions similar to those described using **1**, thus allowing experiments involving these two systems to be studied under comparable conditions.

The growth of AuNPs as a function of irradiation time was monitored by recording the gold SPB, which is displayed at ∼520 nm for 15 nm diameter particles dispersed in aqueous solutions according to Mie theory.[2] The time evolution of the visible SPB is the only direct "real-time" reporter of changes for the systems using I-2959 as the initiator, since I-2959 absorbs strongly in the 320 nm region where Au(III) has a characteristic absorption. In contrast, benzoins **1** and **2** possess minimal absorbance around 320 nm and thus revealed changes in the Au^{3+} ligand-to-metal charge-transfer (LMCT) band centered at 320 nm in CTAC.[34] The growth of the SPB with time is presented in Figure 1 for a deaerated sample containing **1**. It should be noted that the disappearance of the Au(III) band in the 320 nm region precedes the formation of the plasmon band; the absorption decays, reaching a minimum after 2 min, and then increases again. At this point, the sample is probably rich in Au(I). The first significant SPB absorption occurs after 3 min. Not surprisingly, no isosbestic point is observed, given the complexity of the processes leading to the formation of AuNPs.

A comparison of the growth of AuNPs obtained using the three benzoin-derived unimolecular precursors is shown in Figure 2. It is evident that all three precursors offer rapid particle generation, with growth reaching completion within 10 min of UVA irradiation.

(30) Scaiano, J. C.; Abuin, E. B.; Stewart, L. C. *J. Am. Chem. Soc.* **1982**, *104*, 5673.
(31) Eustis, S.; Krylova, G.; Eremenko, A.; Smirnova, N.; Schilla, A. W.; El-Sayed, M. *Photochem. Photobiol. Sci.* **2005**, *4*, 154.
(32) Daniel, M.-C.; Astruc, D. *Chem. Rev.* **2004**, *104*, 293.
(33) Torigoe, K.; Esumi, K. *Langmuir* **1992**, *8*, 59.
(34) Vogler, A.; Kunkely, H. *Coord. Chem. Rev.* **2001**, *219*−*221*, 489.

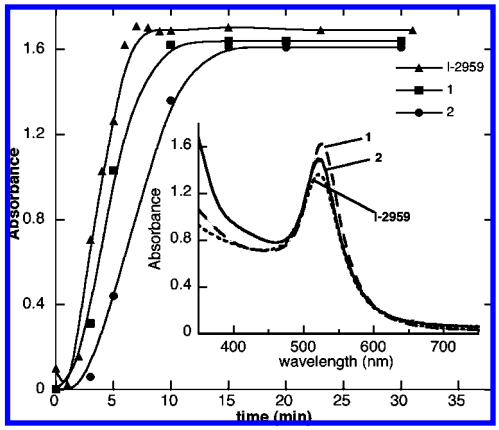

Figure 2. UV−vis absorbance of AuNPs derived from deaerated solutions of I-2959, **1**, and **2** recorded at the corresponding SPB maximum as a function of time for samples containing 1.0 mM ketone, 0.3 mM $AuCl_4^-$, and CTAC concentrations of 17 mM for I-2959 and 66 mM for ketones **1** and **2**. The inset shows representative spectra recorded after exposure for 30 min.

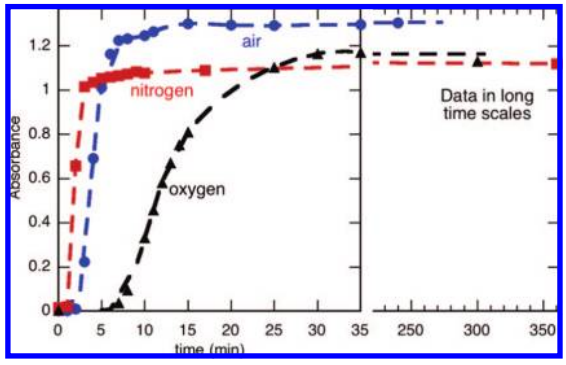

Figure 3. Absorbance changes at the SPB maximum during photolysis of three aqueous solutions containing 0.3 mM $AuCl_4^-$ and 1.0 mM I-2959. Samples were under air (blue) or purged with N_2 (red) or O_2 (black) for equivalent periods of 30 min. The samples were not stirred during UVA exposure. The first 35 min are displayed in detail, while the split panel on the right shows data for $t > 230$ min.

The effect of oxygen on the rate of formation of AuNPs was also studied for the three unimolecular precursors. In all cases, evolution of the plasmon band is slower in the presence of oxygen, an effect attributed to the fact that a fraction of the radicals react with oxygen, which is an excellent radical scavenger.[35] Figure 3 illustrates this observation for the case of I-2959 in water. The zeta potential for particles grown under air was typically around −30 mV and was relatively constant for irradiation times longer than 5 min; the zeta potential values were somewhat more negative in the early stages of UVA exposure. X-ray diffraction (XRD) studies confirmed the crystalline nature of these AuNPs (see the Experimental Section and the Supporting Information for more details about the XRD studies).

It should be noted in Figure 3 that the growth of the SPB starts within 2 min of irradiation time for deaerated samples, whereas a longer delay and slower growth are apparent under ambient conditions. While the induction period represents the time required for the reduction of the aurous acid and sequential nucleation of gold atoms, this period also incorporates the time required to chemically remove molecular oxygen from the system. Previous work by us and others has demonstrated that the benzoyl and ketyl radicals generated from ketone α-cleavage can be quenched by oxygen at near diffusion-controlled rates ($>10^9$ M^{-1} s^{-1}) to give peroxyl radicals or $HO_2\bullet$[35] and hence act as sacrificial oxygen scavengers. At ambient temperature and pressure, the concentration of dissolved oxygen in aqueous systems is submillimolar.[36] If each benzoin molecule generates two radicals that are presumably quenched by oxygen, the residual photoinitiator concentration is still in excess of that required to proceed with metal reduction. In all cases, we believe that the reaction is fast enough that oxygen is not replenished during the unstirred exposure. Despite the differences in the induction times and the final absorption intensities of the various systems, a similar growth pattern is observed for nitrogen and air, as indicated by the similar slopes of the growth curves. This implies that once the oxygen has been consumed, these two samples undergo similar growth rates. In the case of a pure oxygen atmosphere, some oxygen may redissolve during the exposure period or during sample transfers to the UV spectrometer, leading to a reduced growth rate. Oxidation of the substituted benzoyl radicals is expected to generate percarboxylic acids upon further oxidation[37] and eventually carboxylic acids that can assist in the stabilization of air-generated particles, where the position of the SPB is stable for over a year. The absence of these stabilizing acids in deaerated solutions can account for the faster flocculation of particles, resulting in a 20 nm red shift along with broadening and hence decreased intensity of the peak within the first 20 min of irradiation.

Furthermore, in the presence of additional oxygen, some quenching of the benzoin triplet may lead to a reduced yield of radical generation, whereby any reduction and nanoparticle growth is a slow process leading to concurrent nucleation and growth that generates large, polycrystalline particles. Conveniently, in our experience, air offers the best balance between rate of growth and particle stability.

Use of Au(I) and Au(III) as Precursors: Time Evolution. The dependence of the kinetics and the characteristics of the generated AuNPs upon the oxidation state of gold was investigated. Experiments with Au(I) were carried out under similar optimized conditions in order to facilitate comparison of the Au(I) and Au(III) results. There is abundant literature on the synthesis of AuNPs employing Au(III), in which $HAuCl_4 \cdot 3H_2O$ is the most common starting material. However, formation of particles starting from Au(I) has rarely been examined.[13,38−40] A recent contribution[38] identifies the photochemical generation of AuNPs from Au(I) complexes of AuCl in dichloromethane. UVC photolysis generates nanoparticles without the need for a reducing agent. Au(I) slowly but spontaneously oxidizes in aqueous solutions, so careful and quick experimental preparation was necessary.

In our investigation, AuNPs were also generated from Au(I) using the benzoin-photogenerated radicals as reducing agents.

(35) Maillard, B.; Ingold, K. U.; Scaiano, J. C. *J. Am. Chem. Soc.* **1983**, *105*, 5095.
(36) Battino, R. *Solubility Data Series: Oxygen and Ozone*; Pergamon Press: Oxford, U.K., 1981; Vol. 7.
(37) Howard, J. A.; Scaiano, J. C. *Oxyl-, Peroxyl- and Related Radicals*; Fischer, H., Ed.; Landolt-Börnstein: Numerical Data and Functional Relationships in Science and Technology—New Series, Group II, Vol. 13D; Springer-Verlag: Berlin, 1984; p 431.
(38) Elbjeirami, O.; Omary, M. A. *J. Am. Chem. Soc.* **2007**, *129*, 11384.
(39) (a) Bergamini, G.; Ceroni, P.; Balzani, V.; Gingras, M.; Raimundo, J.-M.; Morandic, V.; Merlic, P. G. *Chem. Commun.* **2007**, 4167. (b) Corbierre, M. K.; Lennox, R. B. *Chem. Mater.* **2005**, *17*, 5691.
(40) Corbierre, M. K.; Beerens, J.; Lennox, R. B. *Chem. Mater.* **2005**, *17*, 5774.

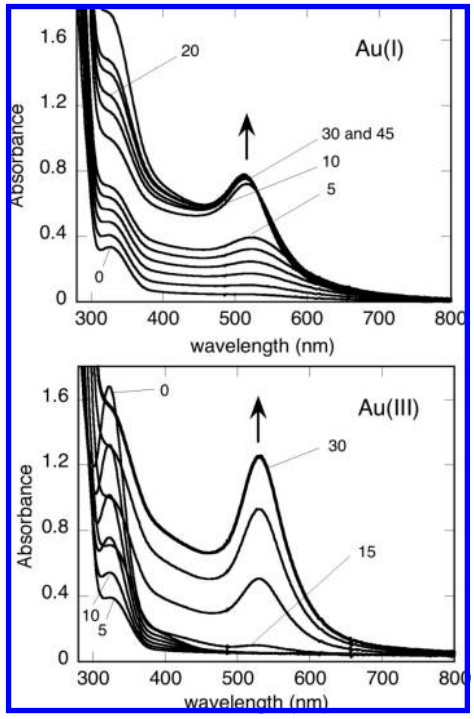

Figure 4. Comparison of the spectral evolutions of deaerated solutions containing 0.33 mM AuCl (top) or $HAuCl_4 \cdot 3H_2O$ (bottom) along with 1.0 mM **2** and 66 mM CTAC. Spectra were recorded at 1 min intervals for the first 5 min and every 5 min thereafter; labels in the graphs show representative exposure times. The spectrum after 45 min (not shown) overlapped with that recorded after 30 min. It should be noted that in the 320 nm region for Au(III), the absorption decays, reaching a minimum after 5 min, and then increases again. The first significant SPB absorption occurs at times just after 10 min. The illuminance was roughly one-half that used in Figure 1.

These experiments were carried out with careful selection of Au(I) precursors, as $AuPPh_3$ and AuCN exhibit high toxicity, which is an undesirable feature for facile and greener nanomaterial synthesis. Furthermore, AuBr was also rejected because of its small extent of dissociation in aqueous media. AuCl was considered to be a better precursor since it overcame these concerns. α-Phenylbenzoin **2** was preferred as the photoinitiator because of its minimal absorbance in the 300 nm region, which allowed us to compare the spectral changes in this area for the two gold salts, as shown in Figure 4. The UV spectrum when AuCl was used (Figure 4, top) revealed that Au(I) was the species in solution, since the characteristic band corresponding to the absorption of Au(III) at ~320 nm was very small; even if some of the 320 nm absorbance is attributed to Au(III), its abundance cannot exceed 15% and is likely much lower. Gold nanoparticles were typically generated from 66 mM CTAC solutions containing 1.0 mM **2** and 0.33 mM AuCl, where dissolution of AuCl was achieved upon sonication of a fresh stock solution in dimethyl sulfoxide (DMSO). Because of the instability of AuCl in various solvents, it was necessary to irradiate the samples promptly after preparation and purging. Irradiation of the sample in a photoreactor generated AuNPs with virtually no induction period, as illustrated in Figure 5. Control experiments were also performed to rule out any effects that DMSO could have had on the rate of growth of the AuNPs (see the Supporting Information).

In order to compare the growth of particles in deaerated solutions of the two oxidation states of gold, their absorbance intensities at the SPB maximum were plotted with time, as

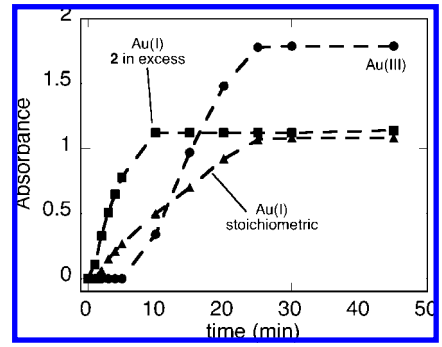

Figure 5. Formation of AuNPs from Au(I) and Au(III). All three solutions were deaerated and contained 0.3 mM AuCl or $HAuCl_4 \cdot 3H_2O$ and 66 mM CTAC; the Au(III) (●) and "excess **2**" Au(I) (■) solutions contained 1.0 mM **2**, while the Au(I) stoichiometric example (▲) contained 0.3 mM **2**. The Au(I) reaction with excess **2** was complete after 10 min, whereas the generation of AuNPs from $AuCl_4^-$ required 30 min.

shown in Figure 5. While the induction period for growth from Au(III) is significantly reduced under deaerated conditions in CTAC, it is essentially absent when the aurous salt is employed. By inspection of the 320 nm peak in the bottom panel of Figure 4, it can be seen that the delay likely corresponds to the consumption of $AuCl_4^-$, leading to $AuCl_2^-$ and eventually Au atoms via reduction and disproportionation. However, the top panel of Figure 4 reveals almost immediate nanoparticle generation, implying that growth occurs from the Au(I) oxidation state. This difference in delay times suggests a stepwise process in the reduction starting from Au(III) in which the reduction of Au(III) to Au(I) is the rate-determining step, as has been confirmed by others.[4,14,33,41]

The stoichiometric ratio of Au(I) and **2** was also investigated. The optimal conditions for Au(III) reduction via the benzoins involve a 3:1 excess of benzoin, which is rationalized via the three one-electron processes required to produce Au(0) prior to AuNP growth. When the same ratio was used with incorporation of AuCl, the intensity of the surface plasmon peak was significantly reduced and the induction period was shorter. This decreased intensity likely corresponds to the decreased concentration of AuCl due to solvent instability and disproportionation; handling AuCl is much more difficult than handling $HAuCl_4$. To verify the concentration of gold in the starting solution, inductively coupled plasma analysis revealed that the starting solution using the AuCl precursor actually contained 33% less gold than the starting solutions containing $HAuCl_4$. When the **2**/Au(I) ratio was changed from 3:1 to 1:1, the formation of AuNP was significantly slower, but approximately the same final SPB absorbance intensity was obtained. The slower AuNP formation in the 1:1 sample is likely due to the reduced absorbance of the initial solution, which simply results in fewer photons being absorbed at 350 nm and hence a lower initial rate for the generation of reducing radicals. Clearly, the stoichiometric requirement of just a one-electron reduction is reflected in the reduced amount of benzoin required.

The characteristic SPB of the AuNPs produced from AuCl has a maximum at 512 nm, whereas that for the particles arising from Au(III) appears at 522 nm, corresponding to larger particles and consistent with the results of transmision electron micros-

(41) (a) Ji, X.; Song, X.; Li, J.; Bai, Y.; Yang, W.; Peng, X. *J. Am. Chem. Soc.* **2007**, *129*, 13939. (b) Kumar, S.; Gandhi, K. S.; Kumar, R. *Ind. Eng. Chem. Res.* **2007**, *46*, 3128. (c) Yonezawa, Y.; Sato, T.; Ohno, M.; Hada, H. *J. Chem. Soc., Faraday Trans. 1* **1987**, *83*, 1559.

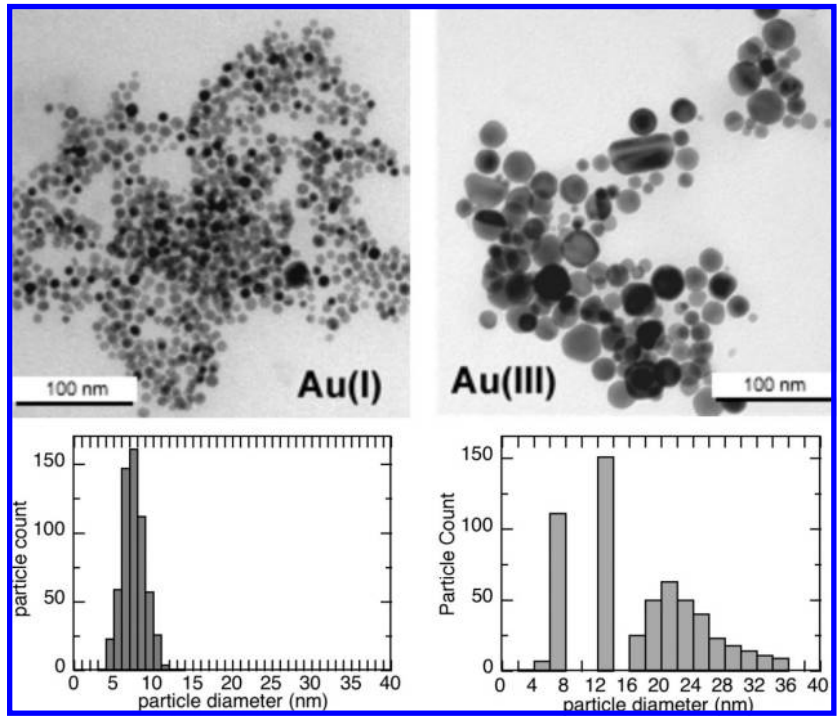

Figure 6. Transmission electron micrographs and particle size distribution histograms for particles prepared as described in the caption of Figure 5: (left) Au(I); (right) Au(III).

copy (TEM) characterization. Both of the AuNP samples show a predominance of spheres with significant polydispersity, as indicated in Figure 6. The corresponding histograms represent particles from Au(I) having diameters of 7.5 ± 1.5 nm and a rather complex distribution of Au(III) particles that formally yields a diameter of 17.0 ± 7.8 nm. The Au(III) distribution is composed of a large group of particles with diameters of ~22 nm and two smaller groups; interestingly, the smallest has essentially the same size as obtained from Au(I). It should be noted that the same horizontal scale was selected for all the histograms shown in this paper.

In both cases, an increase in diameter of ~2 nm was observed within the first two weeks after particle synthesis that is indicative of particle ripening. It should be noted, however (see the Supporting Information), that the distribution narrowed in the case of Au(III) but widened in the case of Au(I). The particle size remained stable for six months thereafter (see the Supporting Information).

Dynamic light scattering (DLS) measurements normally give marginally larger diameters than TEM, consistent with minimal stabilization by small ions, notably chloride. One example of the type of distribution obtained using DLS is shown in Figure S12 in the Supporting Information.

Laser Flash Photolysis Studies of Ketyl Radical Scavenging. Laser flash photolysis techniques allow for the direct detection of short-lived intermediates and their reactions.[42] In our case, the choice of α-phenylbenzoin **2** was largely motivated by the ease of detection of the corresponding benzophenone ketyl radical.[18] Laser flash excitation (λ_{ex} = 355 nm) of deaerated solutions of **2** in acetonitrile gave the characteristic signal of benzophenone ketyl radical (**4**) having two maxima at 325 and 540 nm. Quenching of this signal by gold ions was monitored at 540 nm upon addition of increasing amounts of a DMSO solution of Au(I) (Figure 7, top) or an aqueous solution of Au(III). The pseudo-first-order rate constant for radical decay (k_{obs}) follows eq 1:

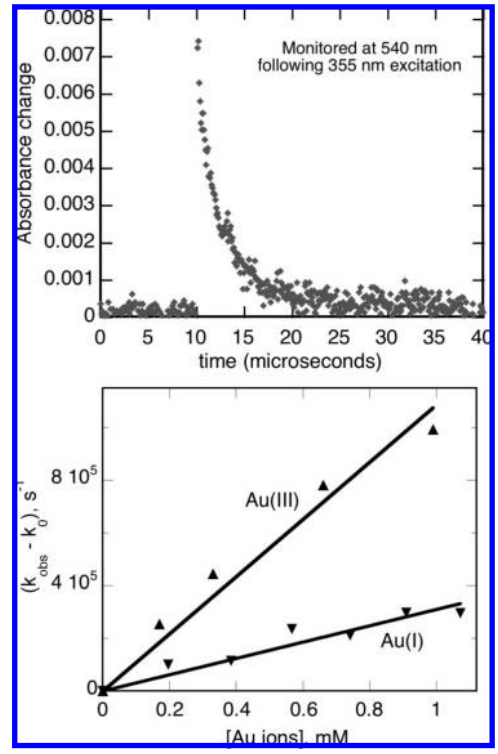

Figure 7. (top) Decay of radical **4** derived from 4.0 mM **2** in deaerated acetonitrile in the presence of 0.6 mM AuCl upon 355 nm excitation at 2 μs. (bottom) Quenching plot of the changes in pseudo-first-order decay rate constants upon addition of AuCl (▼) and $HAuCl_4$ (▲) as radical scavengers.

(42) Scaiano, J. C. In *Reactive Intermediate Chemistry*; Moss, R. A., Platz, M. S., Jones, M. J., Jr., Eds.; Wiley: Hoboken, NJ, 2004; p 847.

$$k_{obs} = k_0 + k_{ET}[\text{Au ion}] \quad (1)$$

where k_{ET} is the rate constant for electron transfer to the scavenger and k_0 is the rate constant for decay in the absence of gold ions, normally determined by reactions with the solvent or impurities in the system (e.g., traces of oxygen). Plots of the pseudo-first-order rate constant for ketyl radical decay as a function of Au(I) or Au(III) concentration (Figure 7, bottom) yielded straight lines whose slopes gave k_{ET} values of 2.5×10^8 and 9.9×10^8 M^{-1} s^{-1} for Au(I) and Au(III), respectively.

Bimolecular Radical Generation. The aromatic ketones in Scheme 3 were selected for this study because they provide a range of behaviors. Benzophenone (**5**) represents the most widely studied ketone, with examples of its photochemistry spanning over a century.[43] Xanthone (**6**) photochemistry is well-understood, and except in hydrocarbon solvents, its triplet state has π,π^* character and thus is relatively unreactive toward hydrogen abstraction, except for truly exceptional donors.[24,44] The triplet spectrum of xanthone is also very sensitive to the solvent polarity, and it has frequently been used as a reporter of this property.[45] In most aromatic ketones, substitution of a phenyl ring with a pyridyl ring increases the n,π^* character of the triplet state and thus its reactivity toward hydrogen transfer; such is the case with 1-azaxanthone (**7**), where the triplet changes to π,π^* character only in pure water, although in micellar solution it still preserves significant hydrogen-abstracting reactivity.[23,26]

Bimolecular Approach to AuNP Generation. Photolysis of aqueous micellar solutions of ketones **5**−**7** in the presence of $HAuCl_4 \cdot 3H_2O$ resulted in nanoparticle formation within minutes, with the rate of appearance of the particle SPB varying with the ketone. In all cases, the growth of particles occurred faster in the absence of oxygen, where the SPBs were also blue-shifted by a few nanometers, suggesting smaller particle sizes. The top panel of Figure 8 shows the SPBs after UVA irradiation for 30 min, while the bottom panel displays the time evolution of the absorbances for **5** and **7** in the absence or presence of oxygen, as measured at the absorbance maximum of the respective SPB. As usual, the delay is longer when oxygen is present.

The reduced rate under aerated conditions is attributed to triplet quenching by oxygen, as oxygen is a known quencher of excited triplet states with rate constants approaching diffusion-controlled values. Quenching implies that fewer chromophores continue on to abstract hydrogen and thus form reducing free radicals. The growth of AuNPs from 1-azaxanthone **7** occurred the fastest of the three ketones studied: the peak growth was complete and stable within 7−8 min. Nanoparticles generated from the ketyl radical of benzophenone **5** also formed efficiently within ~20 min and with a slightly larger yield, as indicated by the plateau absorbance. Xanthone triplets are poor hydrogen abstractors,[24] leading to the formation of fewer ketyl radicals, and thus do not produce particles as quickly. The growth of the SPB when **6** is used is rather slow and was detectable after 30 min of irradiation (Figure 8, top); the plateau was significantly lower than for ketones **5** and **7**. The systems of Figure 8 do not formally contain a hydrogen donor, but reaction can occur by attack at the methylene moieties in the surfactant,[30] as

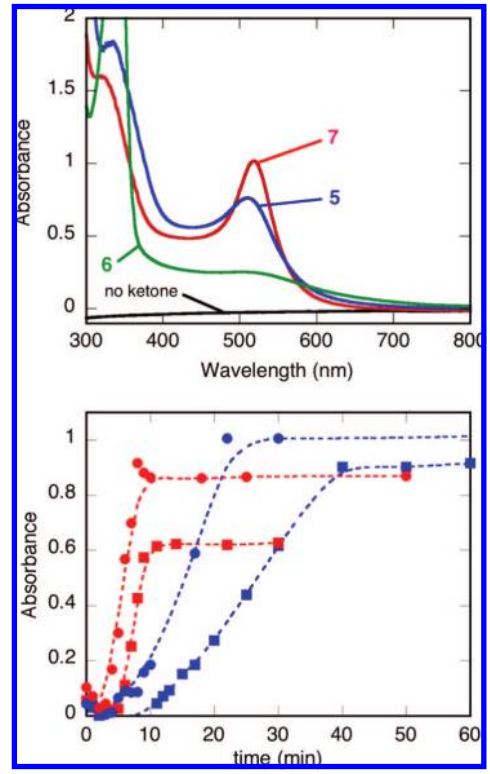

Figure 8. (top) Absorbance spectra representing the generation of AuNPs from aerated solutions containing 17 mM CTAC, 0.3 mM $HAuCl_4$, and 1.0 mM ketone **5** (blue), **6** (green), or **7** (red) after 30 min of UVA irradiation. (bottom) Growth of AuNPs as a function of time for aerated (■) and deaerated (●) solutions containing ketones **5** (blue) and **7** (red).

Scheme 4. Photoreduction of Benzophenone (Triplet) in the Presence of CTAC, Leading to the Formation of Ketyl Radicals

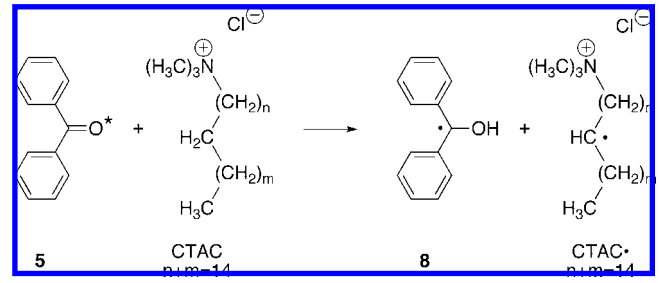

illustrated in Scheme 4 for the example of benzophenone. For the purposes of this work, it is irrelevant which methylene group is involved.

Figure 9 shows a representative example of AuNPs that were grown from benzophenone in deaerated solutions of Au(III) upon UVA irradiation for 30 min. The differences in the behavior observed under various exposure conditions can be attributed to the processes leading to ketyl radical generation from the ketone excited states; we elaborate on these arguments in the Discussion.

With inspiration from previous work involving ketyl radical−metal ion reduction and ketyl radical generation via bimolecular hydrogen transfer with donors such as 1,4-cyclohexadiene,[10] nanoparticle growth studies in the presence of 1,4-cyclohexadiene were also conducted. In all of these experiments, a large excess of 1,4-cyclohexadiene (50 mM) was employed; this ensured that a significant number of 1,4-cyclohexadiene molecules would share the micelles with the ketone. When $HAuCl_4$/ketone samples were irradiated in the presence of 1,4-

(43) (a) Ciamician, G.; Silber, P. *Ber. Dtsch. Chem. Ges.* **1900**, *33*, 2911. (b) Nebbia, G.; Kauffman, G. B. *Chem. Educ.* **2007**, *12*, 362.
(44) Garner, A.; Wilkinson, F. *J. Chem. Soc., Faraday Trans. 2* **1976**, *72*, 1010.
(45) Evans, C. H.; Prud'homme, N.; King, M.; Scaiano, J. C. *J. Photochem. Photobiol., A* **1999**, *121*, 105.

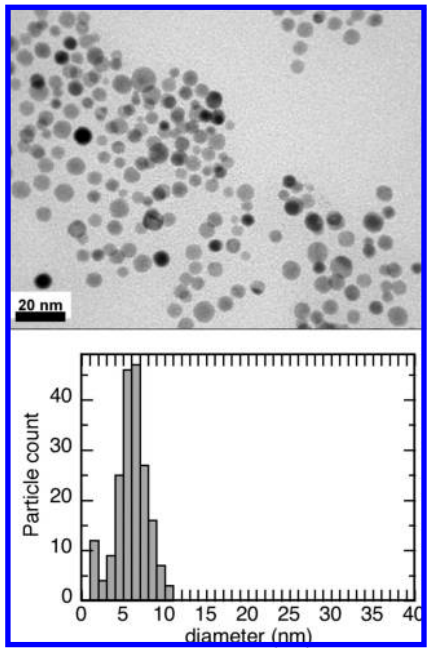

Figure 9. TEM image and particle size distribution of AuNPs grown in deaerated solutions of 0.3 mM $HAuCl_4$, 1.0 mM benzophenone, and 17 mM CTAC upon UVA exposure for 30 min.

cyclohexadiene, nanoparticle growth occurred significantly faster than when the hydrogen donor was the surfactant (as in Scheme 4). In every case, growth with the hydrogen donor was complete in less than one-third the time and with an improved yield compared with AuNP growth without 1,4-cyclohexadiene (see Table 1). Interestingly, however, while the addition of the aromatic donor increased the rate of particle production in deaerated samples compared with that in oxygen-saturated ambient systems, the particle size seemed to increase, as reflected in the positions of the SPBs (Table 1) as well as in the TEM images of the particles obtained from benzophenone in this manner (Figure 10).

The position of the SBP maxima as well as the growth times and plateau absorbances recorded at the SBP maxima for the various micellar systems are summarized in Table 1. The growth times were visually estimated from experimental growth graphs and correspond to ~95% of the maximum (plateau) absorbance achieved in each case.

The choice of 1,4-cyclohexadiene was strategic and based on its ability to donate hydrogen to chromophores with very large rate constants[21,22] to yield reactive allylic radicals. In contrast to conjugated dienes,[46,47] 1,4-cyclohexadiene is not a very good quencher of excited triplet states. A simple comparison was performed using benzophenone under UVA exposure with 1,4-cyclohexadiene or an equivalent amount of its isomer 1,3-cyclohexadiene (Figure 11). While nanoparticles were formed within 5 min using 1,4-cyclohexadiene, no particles were formed within 30 min of exposure time when 1,3-cyclohexadiene was used. Since the two dienes have comparable hydrogen-donor properties,[21] this contrasting reactivity is attributed to the well-known quenching ability of conjugated dienes[46,48] toward excited carbonyls.

In the case of 1,4-cyclohexadiene, the effect is more dramatic with xanthone than with the more reactive ketones. This is illustrated in Figure 12, which compares the ketones studied in micellar solution in the presence or absence of 1,4-cyclohexadiene.

The process by which 1,4-cyclohexadiene works is illustrated in Scheme 5. We note that the ketone is in fact a photocatalyst recovered at the end of the cycle, and thus, this approach may tolerate substoichiometric concentrations of ketone. The fate of the cyclohexadienyl radical was not examined in our work, but it is possible that it contributes to further gold ion reduction, since the aromatization of the cyclohexadienyl radical to form benzene is a highly favorable process.

A common hydrogen donor used in ketone photoreduction is isopropyl alcohol, in a reaction that yields two ketyl radicals. However, addition of isopropyl alcohol was not as favorable as addition of 1,4-cyclohexadiene (see Figure 13), probably reflecting the fact that the ketone resides in the micelle while the alcohol is mostly located in the aqueous phase; notably, the dramatic effect that 1,4-cyclohexadiene has on xanthone (see Figure 12) is not observed for isopropyl alcohol.

Laser Flash Photolysis Studies of Carbonyl Triplet Quenching. The dynamics of some of the key processes involved can be examined using laser flash photolysis techniques.[42] Azaxanthone **7** was selected for these experiments and is anticipated to have a behavior comparable to that of other aromatic ketones. The pseudo-first-order rate constants for triplet decay were measured at different gold concentrations, and the bimolecular rate constants were derived from the slopes of the plots of k_{obs} versus gold concentration (Figure 14). The values obtained are 1.03×10^{10} M^{-1} s^{-1} for Au(III) in 3:1 water/acetonitrile and 2.8×10^{9} M^{-1} s^{-1} for Au(I) in acetonitrile, both determined at room temperature under a nitrogen atmosphere. The data in Figure 14 have been plotted as $k_{obs} - k_0$ because the lifetimes in the absence of quencher were different, reflecting the different solvents and concentrations used in the two experiments. The lifetimes were 5.3 μs for 0.4 mM **7** in acetonitrile and 310 ns for 4 mM **7** in 3:1 water/acetonitrile. The short lifetime in the latter case is likely a reflection of the well-known rapid self-quenching of **7**.[49] Both values are indicative of efficient triplet quenching, the process underlying many of the long exposure times required to prepare AuNP photochemically according to the literature.

Discussion

While gold and other nanoparticles are frequently prepared by thermal methods, a number of photochemical routes have been developed.[7−9,31,32,50,51] Rather frequently, these photochemical routes involve long irradiations and use the same stabilization techniques employed in thermal syntheses. For example, a recent report described the preparation of AuNPs in the dendrimer PAMAM by using benzoin as a precursor and exposure to UVC light for periods as long as 90 min.[7] While the role of benzophenone as a hydrogen abstractor has been

(46) Hammond, G. S.; Saltiel, J.; Lamola, A. A.; Turro, N. J.; Bradshaw, J. S.; Cowan, D. O.; Counsell, R. C.; Vogt, V.; Dalton, C. *J. Am. Chem. Soc.* **1964**, *86*, 3197.
(47) Scaiano, J. C.; Leigh, W. L.; Meador, M. A.; Wagner, P. J. *J. Am. Chem. Soc.* **1985**, *107*, 5806.
(48) Turro, N. J. *Modern Molecular Photochemistry*; Benjamin/Cummings Publishing Co.: Menlo Park, 1978; p 628.
(49) Martinez, L. J.; Scaiano, J. C. *J. Phys. Chem. A* **1999**, *103*, 203.
(50) Pal, A. *Mater. Lett.* **2004**, *58*, 529.
(51) (a) Eustis, S.; Hsu, H. Y.; El-Sayed, M. A. *J. Phys. Chem. B* **2005**, *109*, 4811. (b) Wang, L.; Wei, G.; Guo, C.; Sun, L.; Sun, Y.; Song, Y.; Yang, T.; Li, Z. *Colloids Surf., A* **2008**, *312*, 148.

Table 1. Summary of Spectral Data and Signal Growth Information for AuNPs Produced from Various Intermolecular Ketone Precursors in the Presence or Absence of Air and 1,4-Cyclohexadiene (1,4-CHD)[a]

	benzophenone				xanthone				1-azaxanthone			
	aerated		deaerated		aerated		deaerated		aerated		deaerated	
hydrogen donor	CTAC	1,4-CHD	CTAC	1,4-CHD	CTAC	1,4 CHD	CTAC	1,4-CHD	CTAC	1,4-CHD	CTAC	1,4-CHD
growth time (min)	40	7	22	7	58	3	90	2	11	3	7	2
SPB maximum (nm)	524	538	519	529	526	531	528	517	517	531	511	532
absorbance at plateau	0.95	1.0	1.0	1.2	1.0	1.0	0.45	0.82	0.62	1.0	0.87	1.2

[a] Experiments using 1,4-CHD as the hydrogen donor also took place in the presence of CTAC micelles.

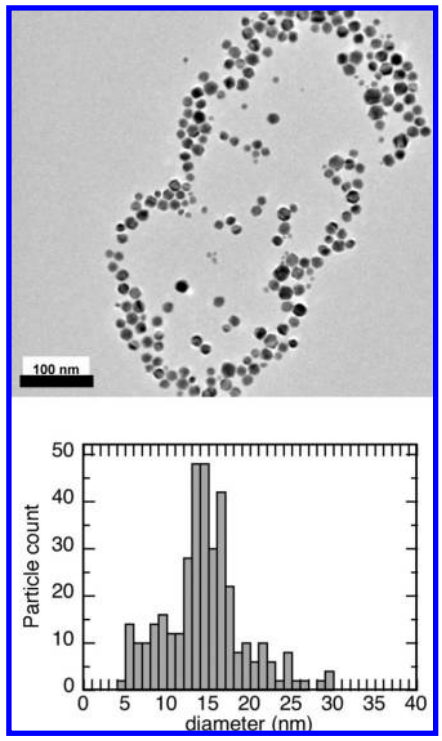

Figure 10. TEM image and particle size distribution of AuNPs formed from 30 min UVA photolysis of a deaerated solution of 0.3 mM $HAuCl_4$, 1.0 mM benzophenone, and 50 mM 1,4 cyclohexadiene in 17 mM CTAC.

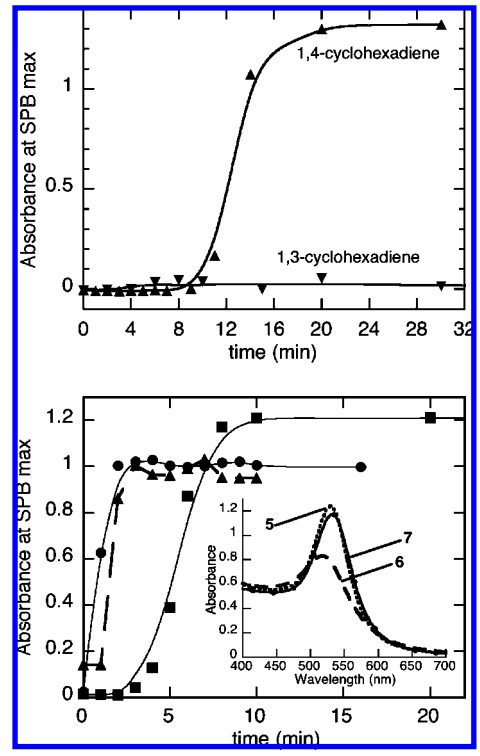

Figure 11. (top) Growth of AuNPs in deaerated solutions containing 0.3 mM $HAuCl_4$, 1.0 mM benzophenone, and 50 mM 1,4-cyclohexadiene (▲) or 1,3-cyclohexadiene (▼) in 17 mM CTAC; the latter diene shows no particle formation. (bottom) Growth of AuNPs from deaerated samples containing 0.3 mM $HAuCl_4$, 1.0 mM ketone **5** (■), **6** (▲), or **7** (●), and 50 mM 1,4-cyclohexadiene in 17 mM CTAC. The inset shows their absorbance spectra after UVA irradiation for 30 min.

recognized, the fact that abstraction from alcohols yields two ketyl radicals has occasionally been overlooked.[31] Our studies show the importance of taking into consideration the absorption properties of the precursors, their excited-state lifetimes, the quenching characteristics of the metal ions, the presence of oxygen, and the possible need of hydrogen donors. We note that while our studies center on ketyl radicals, the interaction of other radicals during AuNP formation or with preformed particles has also attracted recent attention.[3,27,28]

Xanthone has an excited state whose character is strongly solvent-dependent and displays n,π^* behavior only in hydrocarbon solvents; in aqueous, alcoholic, or micellar media, the triplet states invert, leading to a lower-energy π,π^* state with significantly lower reactivity toward hydrogen transfer.[24] In contrast, 1-azaxanthone has n,π^* character under most experimental conditions (except pure water)[49] and is highly reactive in hydrogen- and electron-transfer reactions.[26] Both xanthone and 1-azaxanthone show weak fluorescence, particularly in polar media, and are prone to rapid self-quenching.[23,24,26,49,52] The singlet−triplet energy gap in 1-azaxanthone is estimated to be ~6 kcal/mol, and its efficiency of intersystem crossing was previously studied, yielding $\Phi_{ISC} = 0.82$.[26]

The behavior of the ketyl radicals and their electron transfer to gold ions plays a key role in the production of AuNPs; thus, benzophenone ketyl radical (derived from **5**) transfers an electron to Au(I) with a rate constant smaller than that for Au(III). In previous work, the reduction potential of 1-azaxanthone was measured in acetonitrile to be −1.48 V versus SCE.[23] The reduction potentials versus SCE for the three-electron $AuCl_4^-$ and one-electron AuCl reductions are +1.00 and +1.11 V, respectively.[14] This implies that it is more difficult to donate the first electron to stable Au(III), which yields an unstable Au(II) species that rapidly disproportionates to Au(I) and Au(III), than to transfer an electron to Au(I) to yield Au^0. However, both processes are extremely favorable, and rate-constant differences are probably determined by other parameters such as solvation and reorganization energy. From the point of view of AuNP synthesis, it is clear that electron transfer from ketyl radical **8** will be easy whether Au(I) or Au(III) is involved,[14] as the measured rate constants demonstrate. We note

(52) Blake, J. A.; Gagnon, E.; Lukeman, M.; Scaiano, J. C. *Org. Lett.* **2006**, *8*, 1057.

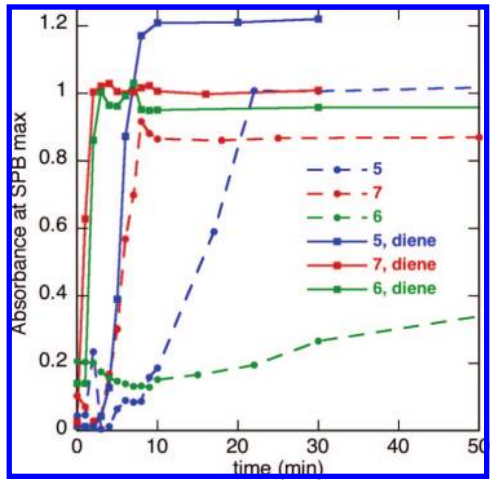

Figure 12. Growth of AuNPs in deaerated samples under UVA exposure in micellar solutions containing 0.3 mM $HAuCl_4$ and 1.0 mM ketone in 17 mM CTAC in the presence or absence of 50 mM 1,4-cyclohexadiene. Colors denote ketones as labeled in the figure; dashed lines correspond to the absence of diene. The lines are for visual help only (i.e., no particular curve fitting was implemented).

Scheme 5. Photoreduction of Benzophenone by 1,4-Cyclohexadiene and Reduction of Gold Ions, Illustrating the Photocatalytic Nature of the Process

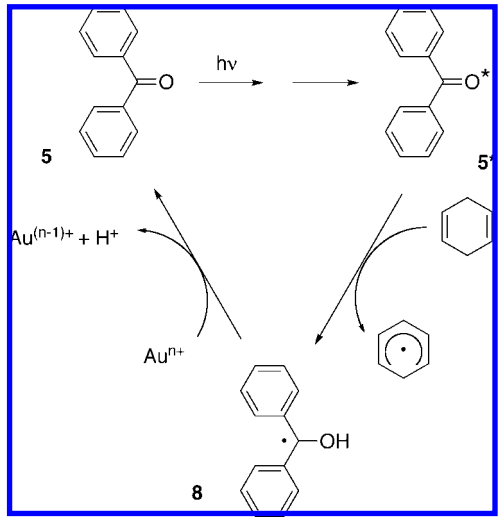

that the reaction will be even more favorable in the case of the acetone ketyl, as generated from I-2959. In fact, the photoreduction of benzophenone in isopropyl alcohol yields benzopinacol (Scheme 6), reflecting the relative electron-donating ability of the two ketyl radicals; indeed, this is a common experiment in introductory organic chemistry.[53]

This work demonstrates how the fundamental paradigms of photochemistry[48,54] can be employed to develop a toolkit for the efficient photochemical synthesis of metal nanoparticles (AuNPs in the examples reported herein). We have not tried to establish ways to make the smallest or most monodispersed particles, as we believe that these strategies are well-developed in the literature[2,32,55] and can be used with the photochemical strategies developed here. If anything, we have tried to minimize the addition of strongly bound stabilizers, such as thiols, not

(53) Tokumaru, K.; Coyle, J. D. *Pure Appl. Chem.* **1992**, *64*, 1343.
(54) Turro, N. J. *J. Photochem. Photobiol., A* **1996**, *100*, 53.
(55) Eustis, S.; El-Sayed, M. A. *Chem. Soc. Rev.* **2006**, *35*, 209.

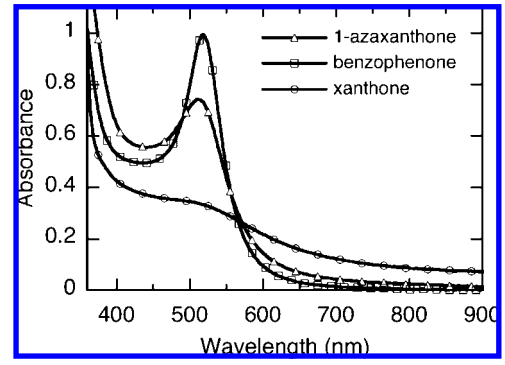

Figure 13. Addition of 0.1 M isopropyl alcohol in the presence of 0.3 mM $HAuCl_4$, 1.0 mM ketone, and 17 mM CTAC has little or no effect on the photochemical consequences of photoinduced AuNP formation, as absorbance and growth dynamics identical to those in the presence of CTAC alone as a hydrogen donor are observed.

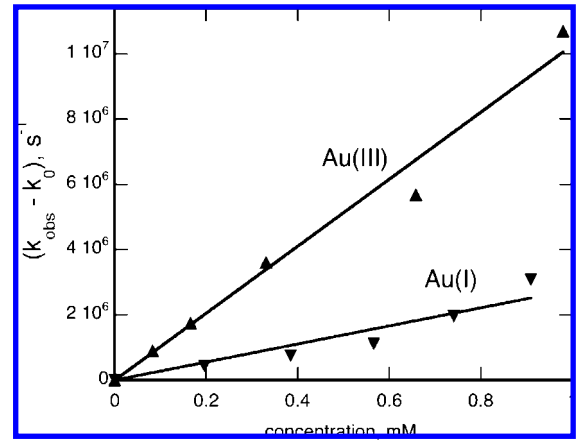

Figure 14. Quenching of triplet **7** by gold ions. In the case of Au(I), the samples contained 4.0 mM **7** in nitrogen-purged acetonitrile; Au(I) was added from a fresh stock solution of AuCl in acetonitrile. The samples in the Au(III) study contained 0.4 mM **7** in 3:1 water/acetonitrile. Laser flash photolysis was performed with 355 nm excitation.

Scheme 6. A Common Synthesis of Benzopinacol Illustrates the Relative Electron Donor Properties of the Acetone and Benzophenone Ketyl Radicals

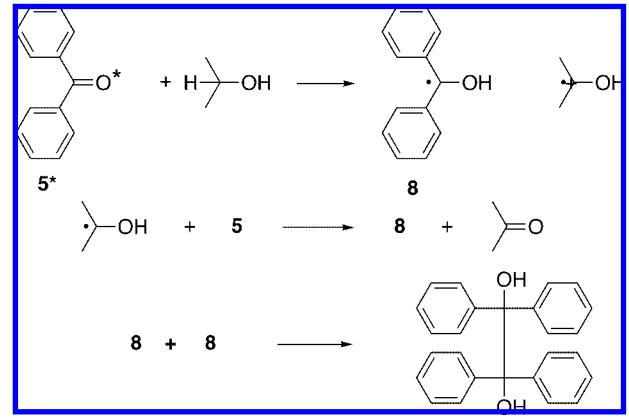

because we fail to see their value, but rather, as in earlier work,[9] because we feel that the unprotected or mildly stabilized particle is the best precursor for custom-modified particles required to meet a specific need. We have, however, been able to make nanoparticles in the 8−50 nm range under controlled conditions and ones as large as 300 nm (unstable) by prolonged ambient exposure (cool white lamps containing up to 3% UVA light).

Smaller particles may be accessible if higher irradiances than those used here (i.e, >100 W/m^2) are employed.

It is important to note that *ketones are good sensitizers for nanoparticle synthesis not because of the energy they can deliver but rather because of the free radicals they can generate*. The following summary in list form provides an outline of the strategies developed here:

(1) Ketyl radicals are excellent reducing agents, forming in the process relatively mild products, such as acetone in the case of I-2959. In the case of gold, the process is favorable for all relevant oxidation states.[14] It should be noted that reaction with ketyl radicals normally generates acid as well, and therefore, pH adjustment may be necessary if the system under study cannot tolerate a pH reduction. Preliminary work with sources of α-aminoalkyl radicals, which are also excellent reducing agents,[56] has suggested that these precursors are prone to thermal reduction of Au(III).

(2) Precursors and excitation sources must be selected to avoid excitation of other components. This is particularly true for Au(III) salts, in which case the most common precursor ($HAuCl_4$) shows a strong absorption at ~320 nm and significant absorptions at shorter ultraviolet wavelengths. In our experience, UVA light (315−400 nm) is most useful. The emission of common UVA lamps is centered at ~350 nm, which is probably the most useful region for the purposes of this work.

(3) In the case of unimolecular precursors, benzoin derivatives such as those in Scheme 1 have proven most useful, since they generally meet the key requirement of short triplet lifetimes (10 ns or less being common).[17] This minimizes triplet quenching by metal ion precursors. Generally, ketones with low lying n,π^* states have shorter triplet lifetimes.[57] The quantum yields of decomposition are frequently in the 0.2−0.4 range, which is quite adequate for this purpose. The solubility of benzoins can be readily tuned by appropriate ring substitution, and several (e.g., I-2959) are commercially available since they are useful initiators for vinyl polymerization.

(4) Ketones that do not undergo Norrish type-I cleavage to yield ketyl radicals are not good precursors unless their excited-state behavior is "tuned" in order to form reducing radicals. For ketones with intrinsic triplet lifetimes of several microseconds, their most common fate in the presence of gold ions is unproductive quenching, leading to the need for long exposure times. The strategies described here provide some procedures for avoiding this quenching, a process that is also common with other metal ions.[10,11]

(5) Spatial segregation provides a simple approach for reducing unproductive triplet-state quenching. Numerous self-assembled nanostructures could be used for this purpose; the key requirements are transparency in the UVA region and the absence of structural groups that could cause unproductive quenching. Micelles provide a simple nanoreactor for this purpose. CH_2 sites can in fact be reactive (see Scheme 4), leading to desirable ketone-derived ketyl radicals. We note that triplet ketones in micelles are not immune to metal ion quenching, as we have shown in the case of silver.[10] Coulombic interactions can enhance or reduce this effect, depending on surfactant and precursor charges.

(6) Ketones with low-lying n,π^* triplet states are far more reactive in hydrogen abstraction reactions that those involving π,π^* states.[57] Thus, in our examples, we specifically included xanthone to illustrate the case of a ketone with a low lying π,π^* state. Figure 8 shows that when only a modest hydrogen donor is available (such as the surfactant), xanthone is outperformed by both 1-azaxanthone and benzophenone. Importantly, many triplet ketones are subject to self-quenching, leading to lifetime reductions as the concentration increases,[24,26,49] so the choice of ketone and its concentration should also reflect a consideration of this phenomenon.

(7) The addition of good hydrogen donors can greatly increase the yield of ketyl radical formation. In the case of micellar systems, a molecule that combines good hydrogen-donor ability with hydrophobic character is best. 1,4-Cyclohexadiene meets these criteria extremely well. The cyclohexadienyl radical is also a good reducing agent, largely driven by its aromatization to give benzene, and may contribute to the reduction of gold ions. Residual 1,4-cyclohexadiene or benzene are sufficiently volatile that they can be readily eliminated after the synthesis is complete. We note that alcohols such as isopropyl alcohol are also good hydrogen donors (but not as good as 1,4-cyclohexadiene)[21] and could also be used, although their partition in micelles is likely to favor the aqueous phase.

(8) While "segregation" facilitates the photochemical reactions that produce reducing radicals, it is clear that Au(0) formation cannot occur until the gold ions and the organic reagents (especially transient reagents such as free radicals) effectively get within reaction distances, which for electron-transfer processes essentially means contact distance. Thus, adequate traffic needs to be achieved; ketyl radicals seem to have the right properties for this role, given the alcohol moiety that assists with their aqueous compatibility. Some of the reactions may take place in the micellar Stern layer, which is rich in counterions and accessible from the micellar surface.

(9) Oxygen plays a dual role. Its role as an excited-state quencher may lead to a rate reduction when excited states have relatively long lifetimes as well as to the sacrificial consumption of some free radicals that may react with oxygen in competition with their electron-transfer reactions with gold ions. This inhibition (see Figures 3 and 8) is limited by the low solubility of oxygen in water[36] and the fact that the short reaction times inhibit replenishing of the oxygen in unstirred solutions. While reactions always reach completion earlier in deaerated solutions, the quality of the particles, as measured by their long-term stability, seems to improve when air is present, probably as a result of the formation of stabilizing organic molecules, such as carboxylates, in systems involving Norrish type-I cleavage.

(10) The two photochemical approaches presented here (Norrish type I and photoreduction) do not need to be viewed as totally separate cases. Thus, while substituted benzoin photolysis does not require the use of micelles,[9] this remains a convenient tool for overcoming solubility problems. Similarly, photoreductions could be performed in homogeneous media if the solvent has suitable hydrogen-donating properties, enabling the problem of gold cation (or, in general, transition-metal cation)[11] quenching to be overcome.

The strategies mentioned above clearly cannot cover all possibilities, but some of the basic principles are clear. Given that in many systems in the literature ketyl radicals are key reducing agents, their efficient formation is paramount if good efficiencies and short irradiation times are desirable. Avoiding both the unproductive quenching of excited-state precursors and the use of sensitizers whose absorption can be masked by the absorbance of gold precursors is essential. Photochemistry readily accomplishes temporal and spatial resolution, charac-

(56) Scaiano, J. C. *J. Phys. Chem.* **1981**, *85*, 2851.
(57) Encina, M. V.; Lissi, E. A.; Lemp, E.; Zanocco, A.; Scaiano, J. C. *J. Am. Chem. Soc.* **1983**, *105*, 1856.

teristics that can be very desirable; these can be achieved using techniques that are less expensive than other successful methods, such as electron-beam lithography.[40]

It is interesting that in retrospect, our earlier photochemical synthesis of AuNPs[9] and the synthesis of AgNPs in micellar solutions[10] can be viewed as examples that illustrate the generality of the paradigm outlined above, including the fact that it is not restricted to gold.

Conclusion

Ketone photochemistry can be used as a method for initiating the synthesis of AuNPs, and the reaction can be completed in minutes under common laboratory UVA exposure conditions. The key to achieving this is to find exposure conditions that involve high-quantum-yield processes leading to the generation of ketyl radicals, which act as strong reducing agents toward Au(III) and Au(I) as well as many other metal ions. In order for these reactions to occur with short exposure times, it is necessary to minimize excited-state quenching by metal ions, which can be accomplished by using radical precursors with very short triplet lifetimes or by physically separating the radical-generating reactions from the electron-transfer steps that lead to metal ion reduction. In our examples, we have employed micelles as the nanoreactors to separate these processes, but clearly, other self-assembled structures could be employed.

In the case of intermolecular reactions, ketones with low-lying n,π^* triplet states should be preferred, since they abstract hydrogen (as needed to generate ketyl radicals) more readily. The necessary "traffic" required to have frequent encounters between metal ions and ketyl radicals seems to be readily achieved with hydrophilic ketyl radicals in micelles but could represent a limitation in other self-assembled structures. The presence of oxygen seems to slightly delay nanoparticle formation but also to generally yield particles with increased stability.

Both Au(III) and Au(I) are good precursors, the latter yielding somewhat smaller particles in shorter times; however, Au(I) salts are not as easy to handle as the usually favored $HAuCl_4$.

Experimental Section

UVA Exposure. The samples were exposed to ultraviolet light in a Luzchem photoreactor equipped with UVA lamps. Typically the unit was operated with six lamps, corresponding to 35−40 W/m^2 with ∼4% spectral contamination (mostly visible and UVB light). Some samples were exposed with a modified experimental arrangement, and in these cases (indicated in the text or captions as appropriate), the illuminance was closer to ∼20 W/m^2 but the excitation spectrum was the same as for the other samples.

Sample Preparation. Aqueous solutions containing 3.3×10^{-4} M $HAuCl_4$, 1.0×10^{-3} M ketone, and 1.7×10^{-2} M CTAC were deaerated using either argon or nitrogen by sequentially purging the headspace and subjecting the sample to vortex stirring every 5−10 min to facilitate the removal of oxygen in the samples; this strategy circumvented the foaming problems that are common with surfactant solutions. Samples were irradiated using 10 × 10 mm, or 7 × 7 mm fused silica cuvettes placed in a Luzchem LZC-4V photoreactor equipped with up to 14 UVA lamps and a carousel to rotate the samples during photolysis. Following irradiation, UV−vis spectra were recorded on a Cary UV-50 spectrophotometer. Samples were also characterized via TEM, where the solutions were diluted to 1.5×10^{-3} M CTAC. Approximately 50 μL of solution was delivered to a carbon-coated copper grid, allowed to evaporate prior to imaging, and subsequently washed with methanol.

Laser Flash Photolysis Experiments. Experiments were carried out in a Luzchem LFP-111 system or in a customized system based on an earlier design[24] but using Luzchem control software. A 0.4 mM solution of 1-azaxanthone in acetonitrile was prepared under deaerated conditions such that it had an absorbance of 0.3 at 355 nm (the laser wavelength). A Nd:YAG laser operating at <25 mJ/pulse with a pulse width of ∼6 ns was used for excitation at a wavelength of 355 nm, and the decay of the triplet state of the ketone was monitored at 600 nm. The signal was quenched by addition of successive aliquots of either $HAuCl_4$ or AuCl in acetonitrile. For reactions involving ketyl radicals, the ketyl radical from benzophenone was monitored at 540 nm.

Optimized Procedure for Gold Nanoparticles Photogeneration Starting from Au(III) or Au(I) Using Unimolecular Precursors. Attempts to dissolve AuCl in different organic media (methanol, ethanol, THF) and aqueous solutions at different pH failed because of readily observable decomposition. Nevertheless, AuCl could (reluctantly) be dissolved in either DMSO or acetonitrile with the assistance of sonication. A solution (4 mL) containing 0.3 mM $HAuCl_4 \cdot 3H_2O$ (from a 10 mM aqueous stock solution) or 0.3 mM AuCl (from a 10 mM solution in DMSO or acetonitrile) and 1 mM α-phenylbenzoin (from a 100 mM solution in acetonitrile) in 66 mM CTAC was stirred for 30 min (until the solutes were dissolved) and transferred to a quartz cuvette. It was then deaerated under a flow of nitrogen (the flow was maintained above the surface rather than bubbled through the solution, and at the same time it was sonicated for 15−20 min; this avoided foam formation). The solution was irradiated in a photoreactor as described above for 30 min. After the irradiation was complete, the solution was transferred to borosilicate vials and proved to be stable for months under dark, ambient conditions. We note that surfactant-free samples are not stable in borosilicate glass;[9] thus, aqueous samples were stored in polycarbonate tubes.

Transmision Electron Microscopy. TEM micrographs were collected at Universidad Politécnica de Valencia with a Philips CM-10 microscope operating at 100 kV and at the University of Ottawa with a high-resolution (HR) transmission electron microscope; TEM and HRTEM studies were performed using a JEOL JEM-2100F field-emission transmission electron microscope equipped with an ultrahigh-resolution pole piece operating at 200 kV.

Dynamic Light Scattering and Zeta Potential. The zeta potential was measured using a Malvern Zetasizer Nano NS. Gold nanoparticles prepared in water at pH 3.0 produced a zeta potential of approximately −30 mV. This suggests the existence of a sufficient level of charge stabilization by negative ions in solution, probably residual chloride ions as well as anions of carboxylic acid derived from the benzoyl radical of Scheme 1, whose presence was confirmed by GC−MS analysis.

X-ray Diffraction. XRD was performed using a Philips PW3020 diffractometer with Cu Kα radiation ($\lambda = 1.5418$ Å) to assess the crystallinity of the AuNPs obtained via our photochemical methods. A sample of aqueous AuNPs was prepared by irradiating a solution containing 3.3×10^{-4} M $HAuCl_4$ and 1.0×10^{-3} M I-2959 for 30 min with 14 UVA lamps. The solution was then centrifuged and concentrated prior to dropcasting on a zero-background SiO_2 disk, after which the liquid was evaporated under vacuum. The sample was scanned between 30 and 85° at a rate of 1.0 s/step and a step size of 0.015°. The prominent peaks at $2\theta = 37.2$, 44.2, 64.7, 77.4, and 81.6° are characteristic of the fcc phases (111), (200), (220), (311), and a minor peak for (222) was also present.[58] In addition, the Debye−Scherrer equation was employed to estimate the size of the AuNPs in order to ascertain that the dropcast sample had not agglomerated into a bulk film; the fwhm of the (111) Bragg reflection peak corresponded to a particle diameter of ∼14 nm, in agreement with TEM, DLS, and UV−vis data.

Materials. $HAuCl_4$, AuCl, 1,4-cyclohexadiene (97%), and DMSO (99.5%, spectroscopic grade) were purchased from Sigma-

(58) (a) Leff, D. V.; Brandt, L.; Heath, J. R. *Langmuir* **1996**, *12*, 4723. (b) Chen, S.; Kimura, K. *Langmuir* **1999**, *15*, 1075. (c) Kuo, C.-H.; Chiang, T.-F.; Chen, L.-J.; Huang, M. H. *Langmuir* **2004**, *20*, 7820.

Aldrich and used as received without further purification. CTAC (>95%) and CTAB were purchased from Alfa Aesar (Ward Hill, MA) and used as received. Benzoin, benzophenone, and xanthone were also purchased from Sigma-Aldrich but were recrystallized twice in ethanol prior to use. 1-Azaxanthone was obtained from Maybridge and also recrystallized twice in ethanol. 2-Hydroxy-1-[4-(2-hydroxyethoxy)phenyl]-2-methyl-1-propanone (I-2959) was a generous gift from Ciba Specialty Chemicals; it was recrystallized twice in ethyl acetate prior to use. Doubly distilled deionized water was obtained from a Milli-Q system (18 MΩ resistance), while spectroscopic-grade acetonitrile was purchased from Fisher Scientific and used as received.

Synthesis. α-Phenylbenzoin **2** was prepared as described previously, and its physical properties agreed with those in the literature.[59]

(59) Zhou, L.; Zhang, Y.; Shi, D. *Tetrahedron Lett.* **1998**, *39*, 8491.

Acknowledgment. J.C.S., K.L.M., and M.L.M. thank the Natural Sciences and Engineering Research Council of Canada and the Canadian Foundation for Innovation for generous support. K.L.M. acknowledges support from an Ontario Graduate Scholarship. M.L.M. acknowledges the Spanish Ministerio de Educacion y Ciencia for generous support. Technical support from the Electronic Microscopy Service of Universidad Politécnica de Valencia and Dr. Yun Liu and Dr. Tara Kell of the University of Ottawa is also acknowledged.

Supporting Information Available: Details of UVA lamp spectra, preliminary results using other surfactants, control experiments, TEM data and histograms for fresh and aged samples prepared from Au(I) and Au(III), an XRD spectrum, and DLS data. This material is available free of charge via the Internet at http://pubs.acs.org.

JA803490N